Available online at www.sciencedirect.com

SCIENCE DIRECT®

Journal of Molecular Catalysis A: Chemical 203 (2003) 251–266

JOURNAL OF MOLECULAR CATALYSIS A: CHEMICAL

www.elsevier.com/locate/molcata

Characterization of chromium species in catalysts for dehydrogenation and polymerization

A.B. Gaspar, J.L.F. Brito, L.C. Dieguez*

NUCAT-PEQ-COPPE, Universidade Federal do Rio de Janeiro, C.P. 68502, CEP 21945-970, Rio de Janeiro, Brazil

Received 27 December 2002; received in revised form 9 April 2003; accepted 10 April 2003

Abstract

Chromium catalysts, prepared with different chromium contents, supports and precursor compounds, were characterized by O_2 and CO chemisorption, in order to quantify the Cr^{3+} and Cr^{2+} sites, active species to dehydrogenation and ethylene polymerization reactions. Both probe molecules, O_2 and CO, showed to be selective to the chromium active species, Cr^{3+} and Cr^{2+}, respectively, and a valid method to quantify these sites. Distinct chromium species, Cr^{6+}, amorphous Cr^{3+}, crystalline Cr^{3+} and Cr^{2+}, were characterized by XRD, DRS, TPR, FT-IR and DRIFTS in the calcined and reduced catalysts. The distribution of chromium species, which depends on the content, precursor compound and support, was related to the catalytic activity in the dehydrogenation and polymerization reactions. The catalytic activity to cyclohexane dehydrogenation depends on the dispersion of amorphous Cr^{3+} species. The activity in the ethylene polymerization is related to the amount of Cr^{2+}_A and Cr^{2+}_B species. Both sites showed similar activities.

Keywords: Cr/SiO_2; Cr/Al_2O_3; Chemisorption; XRD; DRS; FT-IR; DRIFTS; TPR

1. Introduction

Chromium catalysts supported on silica and on alumina have industrial application in ethylene polymerization and dehydrogenation reactions [1–5]. The active sites for these reactions are Cr^{2+} [6–9] and Cr^{3+} [10–12], respectively. The chromium catalysts for ethylene polymerization, Phillips-type, are prepared by impregnation of an inorganic precursor on silica of high specific surface and volume of pores, yielding catalysts with 1 wt.% or less chromium content. The literature [13–16] suggests that, independently of the precursor, there is not difference in the oxidation state of the chromium with low Cr content, after calcination, being observed mainly Cr^{6+}. Otherwise, in previous works [17,18], we showed that the chromium content and the precursor compound affected largely the chromium species distribution in their calcined and reduced forms.

Chromium supported catalysts are used in the ethane, propane, *n*-butane and isobutane dehydrogenations to the corresponding olefins, in the temperature range of 623–773 K and atmospheric pressure, with high selectivity to alkenes [19]. One of the dehydrogenation reactions of largest commercial interest is the dehydrogenation of isobutane to yield isobutene, which is intermediary for methyl *tert*-butyl ether (MTBE) production. MTBE is added to gasoline to improve the octane number, yielding cleaner burning fuel [20], but the contamination of drinking water and

* Corresponding author. Tel.: +55-21-2562-8358; fax: +55-21-2562-8300.
E-mail address: lidia@peq.coppe.ufrj.br (L.C. Dieguez).

1381-1169/03/$ – see front matter © 2003 Elsevier Science B.V. All rights reserved.
doi:10.1016/S1381-1169(03)00381-9

groundwater by MTBE is causing its elimination as a gasoline additive [21]. However, an important amount of the isobutene is used to produce butyl rubber, polyisobutylene and other specialities [22]. Besides, the oxidative and non-oxidative isobutane dehydrogenation with chromium catalysts still deserve interest in the literature as a model reaction [23–25].

Cr/Al_2O_3 catalysts have been used industrially in dehydrogenation reactions. These catalysts are prepared by impregnation of a chromium compound, usually nitrate, and resulting catalysts with chromium loading in the range of 3–13 wt.% Cr [3]. The chromium is anchored on alumina through the basic and neutral hydroxyls, observed by infrared spectroscopy at 3775 and 3730 cm^{-1} [19]. The additions of potassium to reduce cracking reactions [3] and other supports, such as zirconia [26], have also been studied.

Several factors have influence in the catalytic activity of the chromium catalysts, as the oxidation state, the structure (amorphous or crystalline, chromates or dichromates) and the interaction of the chromium species with the support. These variations depend on the metallic content, the precursor compound of chromium, the support characteristics and calcination conditions [2,3]. In the calcined state, the presence of Cr^{6+}, with different interactions with the support, and crystalline or amorphous Cr^{3+} have been studied by influencing in the formation of active species in the polymerization and dehydrogenation reactions [1–3,12–14,17–19]. The literature reports that the active site in the dehydrogenation is the Cr^{3+} species coordinated to the hydroxyls, coordinatively unsaturated [10–12]. This species can be obtained by reduction of the calcined sample with H_2 at 773 K. On the other hand, the active site of chromium for ethylene polymerization was reported to be the Cr^{2+} [2,6–9,27]. These sites can be obtained by reduction of the calcined sample with carbon monoxide at 623 K [28]. The reduction with carbon monoxide converts Cr^{6+} toCr^{2+}, while with H_2 only Cr^{3+} is obtained. Moreover, the Cr^{3+} originally present is not reduced [17].

The characterization of the chromium sites of the calcined and reduced states has been studied by using different spectroscopic techniques, like XPS, DRS and FT-IR [2,8,17,29–31]. However, the presence of different surface chromium species hinders the interpretation of the spectra. Particularly, in the analysis of X-ray photoelectron spectroscopy (XPS), the photoreduction of the Cr^{6+} species, induced by the exposition to the X-rays, requires the use of procedures to minimize this effect in order to validate the results [29–31]. The application of adsorption techniques of probe molecules, that allows to quantify the chromium sites, is not very explored and the methodology is not consolidated [12,18,32,33].

The literature reports the use of the chemisorption of O_2 at low temperatures to quantify the Cr^{3+} sites in the bulk or supported Cr_2O_3 [12,32]. Even so, the selectivity of the chemisorption of O_2 to the amorphous sites Cr^{3+} requires more detailed studies. On the other hand, the Cr^{2+} is reported as the active site for ethylene polymerization in Cr/SiO_2 catalysts, being characterized by adsorption of carbon monoxide at room temperature [33], followed by infrared spectroscopy analysis. The Cr^{2+} sites are divided in Cr^{2+}_A, Cr^{2+}_B and Cr^{2+}_C species [6,7,27], in decreasing order of interaction with the hydroxyls groups on the surface of the support, according to the schematic representation of Kim and Woo [27], as showed in Fig. 1. The Cr^{2+}_A and Cr^{2+}_B species are reported to be active in the polymerization, being Cr^{2+}_A the most active [7,8]. Both species adsorb carbon monoxide at 298 K, while the Cr^{2+}_C

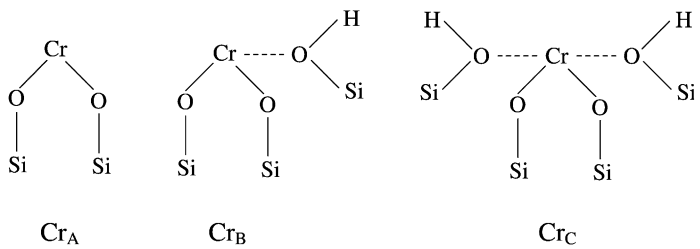

Fig. 1. Cr^{2+} species: Cr^{2+}_A, Cr^{2+}_B and Cr^{2+}_C [27].

does not. In a previous work [18], we showed that catalysts with similar Cr_A^{2+} amount presented different activities in the ethylene polymerization. Our results suggested that not only Cr_A^{2+}, but also Cr_B^{2+} sites have activity in the polymerization. The main problem in the identification of the Cr^{2+} sites is its oxidation when in contact with very low concentration (ppm) of oxygen and/or water [34]. Thus, the characterization and the use of these catalysts in the polymerization require the attainment and maintenance of the Cr^{2+} species during the process. Besides, just a small amount of the Cr^{2+} sites can be considered active to the polymerization (less than 1 wt.% Cr) [35,36]. Therefore, the identification and quantification of these species are important to explain the behavior of chromium catalysts in the ethylene polymerization.

The objective of this work was to study the chemisorption of O_2 and CO to quantify the active sites of chromium catalysts and to evaluate the catalytic activity in the cyclohexane dehydrogenation and in the ethylene polymerization in the light of the chromium species characterization. The dehydrogenation reaction was studied with chromium catalysts prepared on silica and on alumina by varying the chromium content. The polymerization reaction was carried out with chromium catalysts prepared with different precursors supported on silica, resulting 1 wt.% Cr. The catalysts were characterized by X-ray diffraction (XRD), Fourier transform infrared spectroscopy (FT-IR), diffuse reflectance Fourier transform infrared spectroscopy (DRIFTS), temperature programmed reduction (TPR) of H_2 and diffuse reflectance spectroscopy (DRS). The active sites for dehydrogenation and polymerization reactions were quantified by O_2 and CO chemisorption, after reduction with H_2 or CO, respectively.

2. Experimental

2.1. Preparation of the catalysts

The catalysts were prepared by impregnation of aqueous solutions (15 ml/g support) with different chromium contents and precursors added to the γ-Al_2O_3 (Engelhard HARSHAW AL3916P, surface area = 191 m^2/g and pore volume = 0.46 cm^3/g) and SiO_2 supports (Davison GRACE 955, surface area = 299 m^2/g and pore volume = 1.6 cm^3/g). The ethylene polymerization was investigated with Cr/SiO_2 catalysts prepared with different chromium precursors. In the preparation of these Cr/SiO_2 catalysts, chromium acetate(II), chromium chloride(II), chromium oxide(VI), all obtained from Aldrich (99.9% purity), and bis(triphenylsilyl)chromate, prepared according to Baker and Carrick [37], were used, resulting samples with 1 wt.% Cr. The bis(triphenylsilyl)chromate salt was solubilized in hexane (Merck) prior to the catalyst preparation. Cr/SiO_2 and Cr/Al_2O_3 catalysts prepared with different chromium contents were studied in the cyclohexane dehydrogenation. Cr/SiO_2 catalysts were prepared using chromium(III) nitrate (Merck) resulting samples with 1.5, 3 and 5 wt.% Cr. In the preparation of the Cr/Al_2O_3 catalysts, an aqueous solution of chromium(III) nitrate (Merck) was also used, with contents in the range of 1.5–9 wt.% Cr. The catalysts were calcined at 773–823 K for 4 h under dry air flow. Physical mixtures were also prepared mixing by careful grinding CrO_3 or Cr_2O_3 (Aldrich, 99.9%) with silica in an agate mortar, resulting the content of 3 wt.% Cr, and CrO_3 with alumina, in the contents of 2 and 13 wt.% Cr.

2.2. Characterization techniques

X-ray diffraction (XRD) measurements were carried out with the calcined samples, employing a Rigaku Miniflex difractometer (voltage: 30 kV and current: 15 mA), equipped with a copper tube (λ = 1.5417 Å) and a graphite monochromator, operated in the step-scan mode 0.05° 2θ per step and counting for 2 s per step.

Infrared spectroscopy experiments were performed on a FT-IR Perkin-Elmer 2000 spectrometer with a resolution of 4 cm^{-1}, in order to observe the change of the hydroxyls region of silica and alumina because of the interaction with chromium. Self supported wafers (~10 mg/cm^2) were pretreated in situ in a cell equipped with CaF_2 window. The samples were submitted to vacuum at 773 K for 1 h before the analyses. FT-IR spectra were obtained rationing the experimental spectra by the background.

The Cr/SiO_2 catalysts with 1 wt.% Cr were also submitted to DRIFTS measurements on a NICOLET Magna IR 760 instrument with a diffuse reflectance accessory equiped with a vacuum cell from Spectratech.

This analysis was carried out to observe the bands in the region at 2500–4000 cm^{-1} ascribed to the interaction of Cr^{2+} species with the surface hydroxyls of the support, after reduction of the samples with carbon monoxide. The bands at 3725 and 3600 cm^{-1}, ascribed to Cr_B^{2+} and Cr_C^{2+} species, respectively, were monitored [27]. The DRIFTS cell was filled with approximately 22 mg of the sample, and the following activation treatment was carried out in situ: helium flow (AGA, 99.999%) at 773 K for 1 h and reduction at 623 K with a 5% CO/He flow (AGA, <2 ppm O_2, <3 ppm H_2O and <1 ppm CO_2) for 1 h. The spectra were recorded with a resolution of 4 cm^{-1} with a DTGS detector, and are presented as the subtraction of the reduced sample spectrum from the dried sample spectrum in the 4000–2500 cm^{-1} region.

Temperature programmed reduction (TPR) of H_2 were performed in a Pyrex U-tube reactor with an on line thermal conductivity detector (TCD). The catalyst (0.5 g) was dried at 773 K for 1 h with argon flow (AGA, 99.99%) and reduced from 298 to 1023 K (10 K/min) with 1.6% H_2/Ar flow. The TCD, connected to a PC computer, allowed to study the reduction profiles of H_2 with the temperature.

Diffuse reflectance spectroscopy (DRS) analyses were done on a Varian Cary 5 UV-Vis-NIR spectrophotometer equipped with a Praying Mantis diffuse reflection device from Harrick. Spectra were taken in the calcined Cr/Al_2O_3 catalysts, in the range of 800–200 nm, in order to observe the distinct Cr^{6+}/Cr^{3+} species distribution. CrO_3 and α-Cr_2O_3 spectra were used as references.

The chemisorption analysis of carbon monoxide in the Cr/SiO_2 catalysts was accomplished in an equipment ASAP 2000-C from Micromeritcs, after reduction of the samples with a mixture of 5% CO/He at 623 K for 1 h. The procedure was followed by chemisorption of carbon monoxide (static method) at 298 K. The Cr/Al_2O_3 and Cr/SiO_2 (prepared with chromium nitrate) catalysts were analyzed by chemisorption of O_2 at 193 K, after reduction with pure H_2 at 773 K for 1 h. The chemisorption temperature was kept by using an isopropilic alcohol with liquid N_2 mixture. The static chemisorption were obtained in the pressure range of 20–200 mmHg. In each analysis, total and reversible adsorption isotherms were obtained. After reduction of the catalyst and vacuum at the reduction temperature, the total isotherm was obtained. Then, the sample was evacuated at the adsorption temperature and the second isotherm was determined, corresponding to the reversible isotherm. The irreversible chemisorption was obtained by the difference average between the total and reversible isotherms or by the extrapolation of the total isotherm to the null pressure.

2.3. Activity measurements

The 1 wt.% Cr/SiO_2 catalysts (100 mg), prepared with different chromium precursors, were submitted to the ethylene polymerization in a Büchi glasuster reactor (2 l) at 358 K and pressure of 22 bar, using 1 l of *n*-hexane (2–3 ppm H_2O) and triethyl-aluminum (molar TEA/Cr ratio = 6.0). Initially, 1 l of purified *n*-hexane and triethyl-aluminum (TEA), just enough to the elimination of residual humidity of the system, were added to the reactor. After that, the catalyst, previously reduced with CO at 623 K, was carefully transferred to the reactor, using a glove bag with inert atmosphere. Then, purified ethylene (<4 ppm H_2O and <2 ppm O_2) was admitted up to the total pressure of 22 bar. After 1 h of reaction, the polyethylene was removed from the reactor, dried to elimination of the solvent and weighed for determination of the activity.

The Cr/Al_2O_3 and Cr/SiO_2 catalysts (0.5 g), prepared with chromium nitrate and different contents, were studied in the cyclohexane dehydrogenation at 773 K and at atmospheric pressure. The reactional mixture was obtained by passing H_2 flow into a saturator maintained at 285 K ($W/F = 0.016$ g min/ml). In these conditions, diffusional effects are neglected. The tests were accomplished in differential reactor conditions, with conversions about 10%. The reduction pretreatments were identical to the used before the chemisorption analyses, in order to obtain the active sites for dehydrogenation and polymerization.

3. Results and discussion

Chromium catalysts, prepared with different contents supported on silica and on alumina, were evaluated in the cyclohexane dehydrogenation. The ethylene polymerization was studied with 1 wt.% Cr on silica, using distinct chromium compounds. The

Table 1
Chromium contents, precursor compounds and codes of the samples

Sample	Support	Chromium precursor	Cr (wt.%)	Reaction
Catalyst				
1.5CrNAl	Al_2O_3	Nitrate (N)	1.6	Dehydrogenation
3CrNAl			2.7	
6CrNAl			6.3	
9CrNAl			8.6	
1.5CrNSi	SiO_2	Nitrate (N)	1.4	
3CrNSi			3.0	
5CrNSi			5.0	
1CrASi	SiO_2	Acetate (A)	0.76	Polymerization
1CrBSi		Silyl chromate (B)	0.75	
1CrCSi		Chloride (C)	0.64	
1CrDSi		CrO_3 (D)	0.80	
Physical mixture				
2CrAlP6	Al_2O_3	CrO_3	1.9	Dehydrogenation
13CrAlP6			13.1	
3CrSiP6	SiO_2	CrO_3	3.0	Dehydrogenation/polymerization
3CrSiP3		α-Cr_2O_3	3.0	

catalytic activity was associated with the chromium species characterization.

Table 1 presents the samples, catalysts and physical mixtures, and the chromium contents, obtained by atomic absorption spectroscopy. The sample code includes the nominal content, the chromium precursor and the support, resulting the sequence XCrYZ, where X: chromium content, Y: chromium precursor and Z: support. In the physical mixtures, the letter P and the oxidation state of the chromium oxide are included.

3.1. Cr/Al_2O_3 and Cr/SiO_2 catalysts for dehydrogenation

3.1.1. Characterization

The XRD results are presented in Figs. 2 and 3. Comparing the X-ray diffractograms of the catalysts with the one of the pure crystalline α-Cr_2O_3, the characteristic bands of this compound are observed in all the Cr/SiO_2, but not in the catalysts prepared on alumina. This result indicates that the alumina hinders the formation of crystalline α-Cr_2O_3 phase or that it disperses the crystals of α-Cr_2O_3 turning them too small to be detected. Such results suggest a better dispersion of the chromium on alumina than on silica. Cavani et al. [1] observed the α-Cr_2O_3 phase with 5 wt.% of chromium on alumina. However, the authors used a support composed by a mixture of three crystalline phases, which may turn easier the formation of the α-Cr_2O_3. The intensity of the characteristic bands of α-Cr_2O_3 increases with the chromium loading in the Cr/SiO_2 catalysts (Fig. 3). This crystalline phase was detected in the 1.5 wt.% Cr on silica (1.5CrNSi), on the contrary of the reported by McDaniel and Welch [13], that just observed this species starting from 2.9 wt.% Cr. However, other authors have observed lower values for the chromium monolayer on silica, in the range of 1.0–1.5 wt.% Cr [19,38,39].

The FT-IR results are presented in the Figs. 4 and 5. The consumption of the surface hydroxyls decreases as the chromium content increases. Such hydroxyls are the isolated ones in the silica (3740 cm^{-1}) and the basic and neutral ones in the alumina (3775 and 3730 cm^{-1}) [14,40–42]. In the Cr/SiO_2 samples, a significant amount of isolated hydroxyls remains even for the greater chromium content. This result agrees with the work of Vuurman et. al. [19]. In the Cr/Al_2O_3 samples, the hydroxyls consumption is more evident. In the 9CrNAl catalyst, prepared with chromium(III) nitrate, the bands ascribed to the basic and neutral hydroxyls are almost indistinguishable. This result

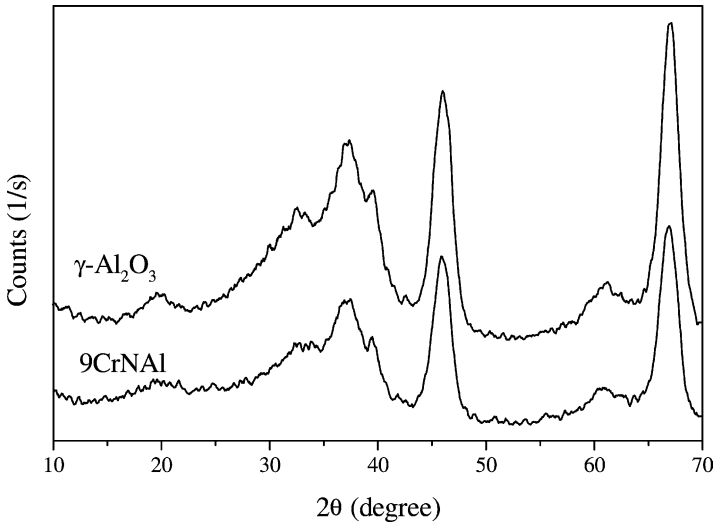

Fig. 2. X-ray diffraction of the Cr/Al_2O_3 catalysts and support.

means an almost complete recovering of the surface of the support. The 13CrAlP6 sample, prepared with chromium oxide(VI), presented an unexpected result. Despite of being a physical mixture, its spectrum did not present the bands of the surface hydroxyls, showing interaction between the support and the CrO_3, as well as a high covering degree. A spreading process must be occurring in this sample. Our hypothesis is based on low surface tension of the CrO_3 and on the hygroscopic characteristic of this oxide. The CrO_3 absorb water from the atmosphere, solubilizes in it and spreads in the surface of the support, as it occurs in the preparation of the catalysts. The 3CrSiP6 sample presented a similar result, with consumption of

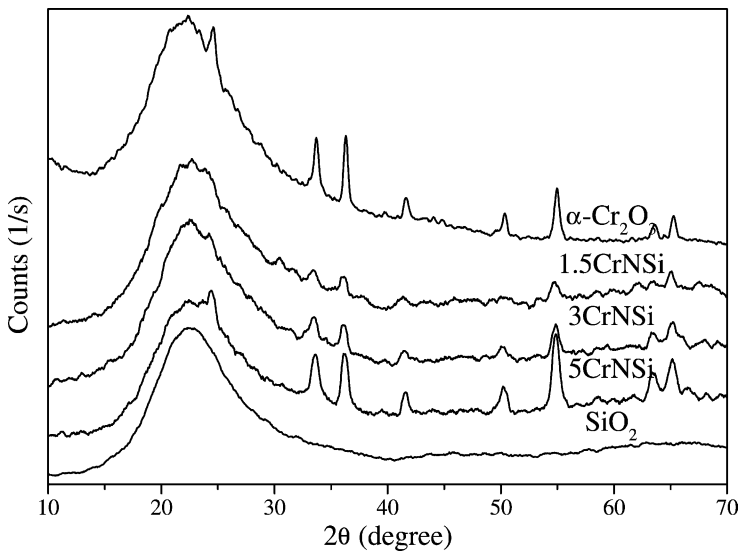

Fig. 3. X-ray diffraction of the Cr/SiO_2 catalysts, support and α-Cr_2O_3.

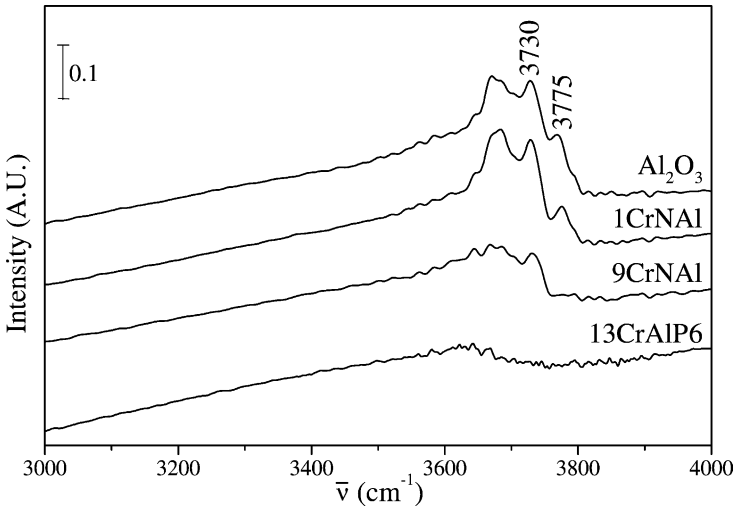

Fig. 4. FT-IR spectra of the hydroxyls region of the catalysts supported on alumina, the 13CrAlP6 physical mixture and the support.

surface hydroxyls greater than would be expected for a physical mixture.

Temperature programmed reduction with H_2 was done to study the chromium-support interaction and to calculate the fraction of Cr^{6+} in the calcined catalysts. Consumption of H_2 was not observed for α-Cr_2O_3. The physical mixtures of CrO_3 with SiO_2 and with Al_2O_3 presented H_2 consumption corresponded to the theoretical reduction from Cr^{6+} to Cr^{3+}, represented by the reaction $2CrO_3 + 3H_2 \rightarrow Cr_2O_3 + 3H_2O$. These results permitted to use the hypothesis that the final oxidation state of the chromium in the reduction

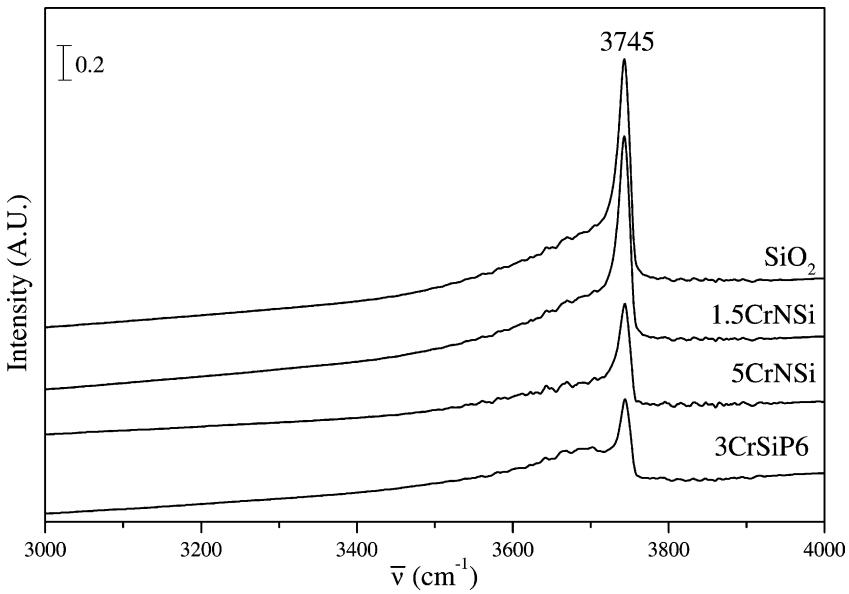

Fig. 5. FT-IR spectra of the hydroxyls region of the catalysts supported on silica, the 3CrSiP6 physical mixture and the support.

Table 2
TPR and XRD analyses results

Catalyst	H_2 consumption[a] (μmol H_2/mg Cr)	T_{max} (K)	Cr^{6+} (%)	α-Cr_2O_3[b]
1.5CrNSi	13.3	756	46	+
3CrNSi	11.3	747	39	+
5CrNSi	2.5	776	9	+
1.5CrNAl	29.7	733	100	−
3CrNAl	23.1	702	80	−
6CrNAl	15.3	678	53	−
9CrNAl	10.7	687	37	−

[a] H_2 consumption for the reduction $Cr^{6+} \rightarrow Cr^{3+}$: 29 μmol H_2/mg Cr.
[b] α-Cr_2O_3 detected (+) or not detected (−) by XRD analysis.

conditions with H_2 is Cr^{3+}. Thus, it was obtained the fraction of Cr^{6+} in the calcined samples, taking into account the theoretical consumption of the reduction from Cr^{6+} to Cr^{3+} (29 μmol H_2/mg Cr) and considering complete reduction of Cr^{6+}.

Table 2 presents the results of H_2 consumption for the Cr/SiO_2 and Cr/Al_2O_3 catalysts, the temperature ascribed to the maximum consumption of H_2 (T_{max}) and the initial percentage of Cr^{6+}. It is observed that the Cr/SiO_2 catalysts presented a smaller H_2 consumption than the theoretical value. This fact can be interpreted as being due to the existence of an initial fraction of Cr^{3+} in the catalysts or as a high interaction of the Cr^{6+} with the support, hindering its reduction to Cr^{3+}. The XRD results confirm the first hypothesis, showing the existence of crystalline α-Cr_2O_3 phase in the three Cr/SiO_2 catalysts after the calcination step, as reported in Fig. 3 and indicated in Table 2. It is also observed a similar H_2 consumption for the 1.5CrNSi and 3CrNSi catalysts, with a marked decrease for the 5CrNSi catalyst. This behavior can be ascribed to the formation of a large fraction of Cr^{3+} in this catalyst and therefore reducing the H_2 consumption. Fig. 6 exhibits the reduction profiles for the Cr/SiO_2 catalysts. It is observed a main peak, in the temperature around 750 K, ascribed to the reduction of Cr^{6+} to Cr^{3+}. The temperatures of maximum consumption of H_2 (T_{max}) were similar, just increasing for the 5CrNSi catalyst. This fact can be interpreted in the same way of the consumption, relative to the formation of crystalline α-Cr_2O_3 phase, that would hinder the reduction of the Cr^{6+} species. Nevertheless, the catalysts also presented H_2 consumption at lower temperature, around 650 K. This behavior can be ascribed to the reduction of Cr^{6+} with different interactions with the support. According to Ellison et al. [43], reduction peaks in the region of 628–678 K in Cr/SiO_2 catalysts are ascribed

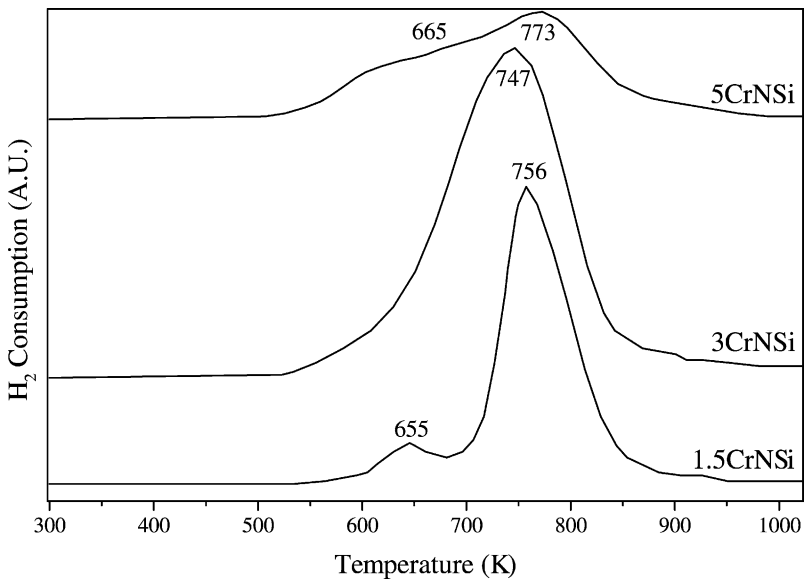

Fig. 6. TPR profiles for Cr/SiO_2 catalysts.

to CrO_3 clusters with smaller interaction with the support.

Concerning the Cr/Al_2O_3 catalysts, the Table 2 shows that for the sample with the lowest chromium content the H_2 consumption corresponds to the stoichometric value for the total reduction of Cr^{6+} to Cr^{3+}. Thus, it was observed only Cr^{6+} in the 1.5CrNAl calcined sample. As the chromium content increases, the catalysts presented decrease in the H_2 consumption. These results are in agreement with the diffuse reflectance spectroscopy (DRS) analyses, shown in Fig. 7. The 1.5CrNAl and 3CrNAl catalysts presented bands at 260 and 380 nm, ascribed to Cr^{6+}, as shown by the CrO_3 spectrum and also reported by Cavani et al. [1]. A shoulder at around 470 nm is also shown, ascribed to Cr^{6+} in the chromate or dichromate arrangement in contact with the support. The increase of the chromium loading caused the appearance of a shoulder at 600 nm in the 6CrNAl and 9CrNAl catalysts, ascribed to Cr^{3+} species, as shown in the α-Cr_2O_3 spectrum. Cavani et al. [1] also observed the initial formation of a fraction of Cr^{6+}, followed by a fraction of Cr^{3+} in Cr/Al_2O_3 catalysts. In this study, the results indicated the initial formation of Cr^{6+} and, later, a growing formation of Cr^{3+}, with increase of the chromium loading. Fig. 8 presents the reduction profiles obtained for the Cr/Al_2O_3 catalysts. Distinctly from the Cr/SiO_2 catalysts (Fig. 6), there is only one peak ascribed to the reduction of Cr^{6+} to Cr^{3+}. Concerning the reduction temperature, it is observed that T_{max} shifts to lower values as the chromium content increases. According to Cavani et al. [1], two Cr^{6+} species, the graftized and the soluble Cr^{6+}, can be formed in Cr/Al_2O_3 catalysts by varying the chromium loading. The observed species in the lower contents is the graftized Cr^{6+}, which presents greater interaction with the support than the soluble Cr^{6+}, formed later. The interaction of the graftized Cr^{6+} with the support would difficult its reduction. As the chromium content increases, a larger fraction of the other species, the soluble Cr^{6+}, easier to reduce, is formed.

Comparing the supports, it is noticed that the catalysts on silica presented thoroughly smaller H_2 consumption than on alumina, besides larger reduction temperature interval and higher maximum temperature (T_{max}). Therefore, the alumina would be capable to stabilize a larger fraction of chromium in the Cr^{6+} oxidation state, or the support would present a smaller interaction with the Cr^{6+}. Both arguments can explain the chromium reduction. These results show that the chromium reduction on silica is more difficult than on

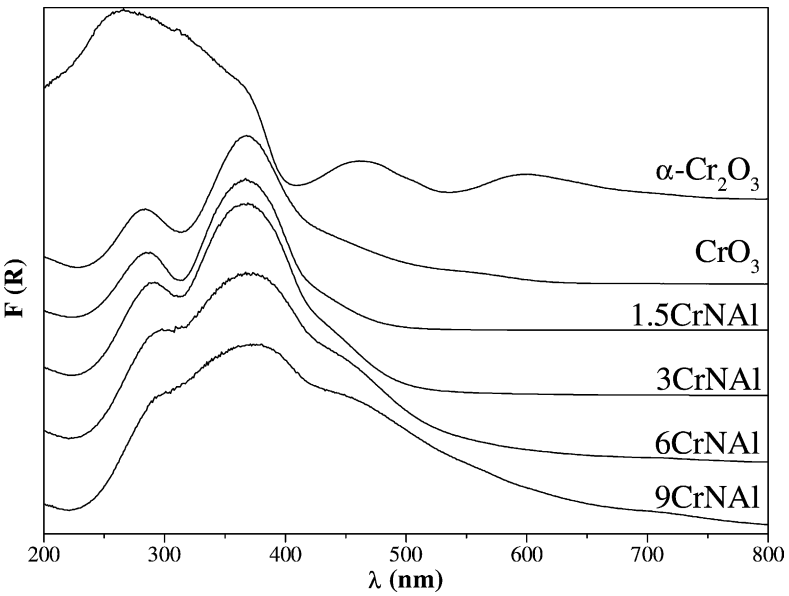

Fig. 7. DRS spectra of the Cr/Al_2O_3 samples, α-Cr_2O_3 and CrO_3.

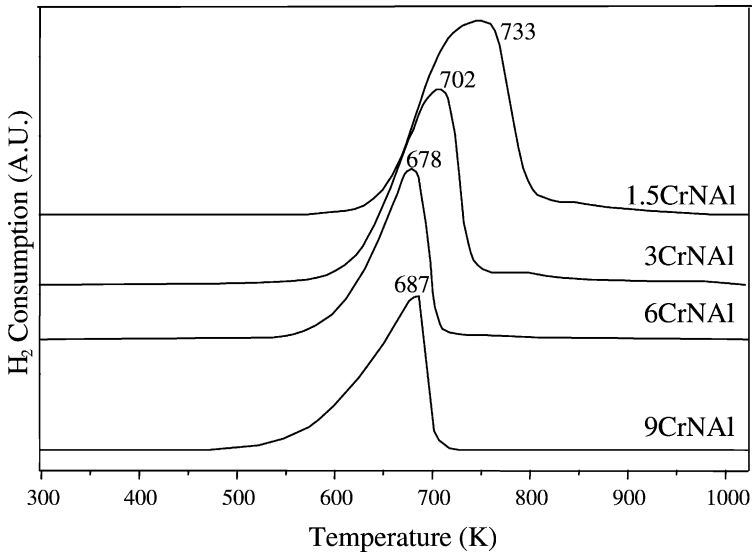

Fig. 8. TPR profiles for Cr/Al_2O_3 catalysts.

alumina, being consistent with the interpretation that the Cr^{6+} interacts more strongly with silica than with alumina.

In order to verify the selectivity of the chemisorption of O_2 to the amorphous Cr^{3+} species, active sites for dehydrogenation [10–12], previous tests were carried out with crystalline Cr^{3+} (α-Cr_2O_3) and CrO_3 in physical mixtures. The tests were carried out after reduction treatment with flow of H_2 at 773 K. The physical mixture with the highest CrO_3 loading (13CrAlP6) was used to verify the occurrence of O_2 chemisorption in the Cr^{6+} sites. In this case, the pretreatment consisted only of drying the sample under He flow at 473 K to avoid the reduction of the Cr^{6+}. These tests are presented in the Table 3. The results of the difference average among the total and reversible values of O_2 (Q_{medium}) of the supports and the physical mixtures (13CrAlP6 and 3CrSiP3) presented deviations in relation to the values obtained for the extrapolation of the total isotherm for null pressure (Q_{P_0}). The isotherms obtained for the 3CrSiP3 physical mixture are presented in the Fig. 9(A). It is noticed that the difference between the total and the reversible isotherms is not constant, increasing with the pressure, phenomenon ascribed to the physisorption [44,45]. Thus, the value of the amount of O_2 chemisorbed corresponds to the extrapolation to null pressure. On the other hand, the isotherms for amorphous Cr^{3+} (2CrAlP6 physical mixture) presented similar values for the total isotherm at null pressure and the average of the difference among total and reversible isotherms, 4585 and 4464 μmol O_2/g Cr, respectively (deviation around 3%). In this case, the discount of the reversible fraction of O_2, guarantees

Table 3
Preliminary tests of O_2 chemisorption

Sample	Chromium species[a]	Q_{medium} (μmol O_2/g Cr)	Q_{P_0} (μmol O_2/g Cr)
13CrAlP6	Cr^{6+}	9	1
3CrSiP3	α-Cr_2O_3	533	237
α-Cr_2O_3	α-Cr_2O_3	34	32
2CrAlP6	Amorphous Cr^{3+}	4585	4464

[a] Characterization by X-ray diffraction (XRD) and temperature programmed reduction (TPR).

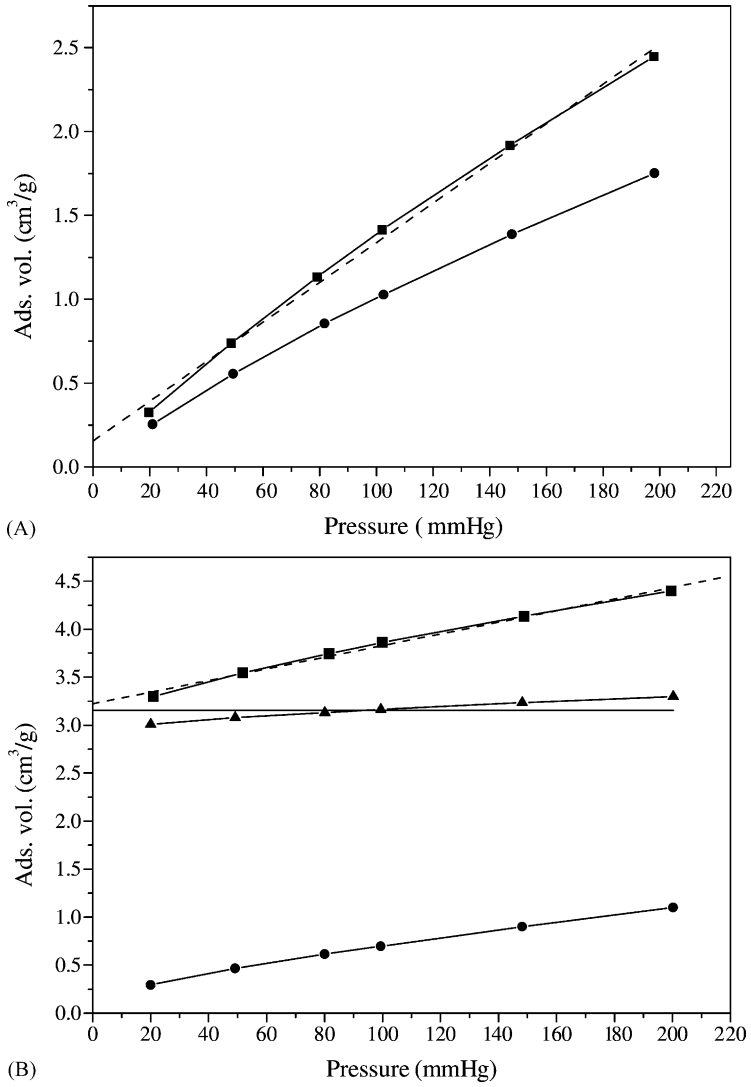

Fig. 9. O_2 adsorption isotherms to the physical mixture 3CrSiP3 (A) and the catalyst 9CrNAl (B). (■) Total isotherm; (●) reversible isotherm; (---) extrapolation to null pressure; (▲) total-reversible difference; (—) difference medium.

the reliability of the irreversible amount. The same behavior was verified for all the catalysts, exemplified in the Fig. 9(B) for the 9CrNAl catalyst.

With the results of Table 3, it was possible to confirm that the Cr^{6+} practically does not chemisorb O_2 in comparison with the amorphous Cr^{3+}. The crystalline Cr^{3+}, bulk or in physical mixture with the support, chemisorb in small amount. However, α-Cr_2O_3 chemisorbs seven times more oxygen in physical mixture than in the bulk, 237 and 32 μmol O_2/g Cr, respectively, ascribed to the dispersion process of the chromium with the support. The result found by Rama Rao et al. [12] for a bulk α-Cr_2O_3 (34 μmol O_2/g Cr) was similar to that found in this study (32 μmol O_2/g Cr). Nevertheless, in both cases the chemisorbed amount in the crystalline Cr^{3+} is small in comparison with the amorphous Cr^{3+}. The chemisorbed amount in the amorphous Cr^{3+} (2CrAlP6) is about 20 times greater than for α-Cr_2O_3 in physical mixture, what means that O_2

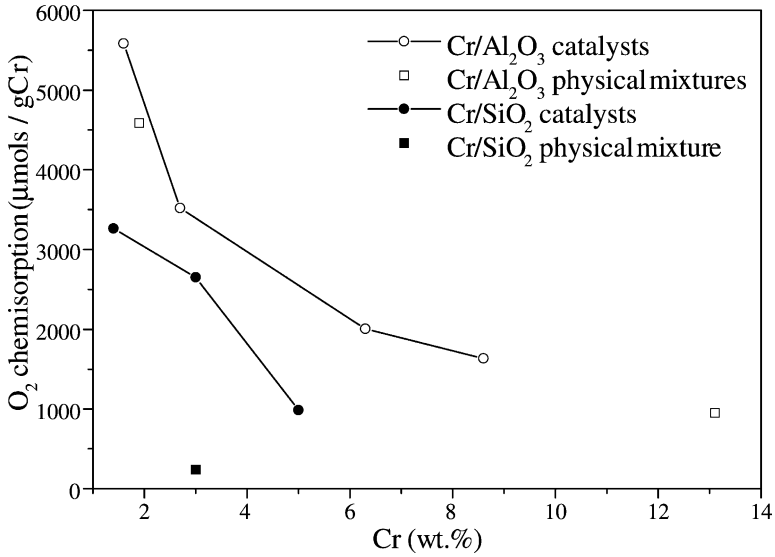

Fig. 10. O_2 chemisorption versus chromium content for samples supported on alumina and on silica.

chemisorption occurs predominantly in the amorphous Cr^{3+}.

The Cr/SiO_2 and Cr/Al_2O_3 catalysts were analyzed by O_2 chemisorption with the aim of study the effects of the chromium content and of the support in the active sites for dehydrogenation reaction. The Fig. 10 shows that both Cr/Al_2O_3 and Cr/SiO_2 catalysts presented a decrease of the O_2 chemisorption as the chromium content increases. It is also observed that the physical mixtures of CrO_3 on Al_2O_3 presented values of O_2 chemisorption with the same tendency of the catalysts, depending on the chromium content of the samples. This behavior is not the expected for simple physical mixtures. The result of the 2CrAlP6 sample is significant to analyze this subject. This sample presented a value for O_2 chemisorption between 1.5CrNAl and 3CrNAl catalysts. As discussed for the FT-IR analysis of the 13CrAlP6 physical mixture, this result can also be ascribed to a spreading process driven by the extremely hygroscopic characteristic of CrO_3. This spreading phenomenon can also be influenced by the characteristics of the support. As the CrO_3 is an oxide with acidic character, it interacts with the basic hydroxyls of the alumina and this process is promoted by its low surface tension [46].

Table 4 presents the measurements of O_2 chemisorption after the reduction treatment. The results show a decrease of the amount of O_2 chemisorbed with the increase of the chromium content. The data were interpreted as an increase of the aggregation of the particles of chromium for higher contents. For Cr/SiO_2 catalysts, another factor is that the decrease of the value of O_2 chemisorption is consequence of the formation of the crystalline α-Cr_2O_3 phase, detected by XRD (Fig. 3), which does not chemisorb O_2 and whose proportion would increase with the chromium content [1].

It is also observed that the results of O_2 chemisorption for the samples on alumina were systematically greater than on silica, which suggests a better capacity of the alumina to disperse the active phase. This phenomenon is connected to the higher concentration of the surface hydroxyls of alumina in comparison to the silica. The concentration of the surface hydroxyls is estimated to be about 6.7 OH/nm^2 in the silica and 12.6 OH/nm^2 in the alumina at 373 K [38,39]. The chemisorption results were coherent with the XRD analyses, which showed a crystalline α-Cr_2O_3 phase on silica whose intensity increased with the chromium content. This fact, once the crystalline Cr^{3+} does not chemisorb O_2, provokes a decrease in the amount of O_2 chemisorbed by chromium loading. On the other hand, crystalline phase was not found in the catalysts supported on alumina, Fig. 2, justifying that the

Table 4
O_2 chemisorption and cyclohexane dehydrogenation for supported Cr/Al_2O_3, Cr/SiO_2 and physical mixtures

Sample	Chemisorption (μmol O_2/g Cr)	$-r_{CH}$ ($\times 10^3$) (mol cyclohexane/g Cr min)	TON ($\times 10^3$) (s^{-1})
1.5CrNSi	3262	1.08	2.8
3CrNSi	2651	1.47	4.6
5CrNSi	987	–	–
3CrSiP3	237	NA[a]	NA
1.5CrNAl	5585	0.99	1.5
3CrNAl	3518	2.21	5.2
6CrNAl	2006	2.60	10.8
9CrNAl	1634	2.79	14.2
2CrAlP6	4585	0.72	1.3
13CrAlP6	954	3.23	28.2

[a] No activity.

results of chemisorption of the catalysts on alumina were larger than on silica. Based on those results, the O_2 chemisorption analysis was considered consistent and a valid method to quantify the amorphous Cr^{3+} sites and, therefore, its results were compared with the catalytic tests.

3.1.2. Cyclohexane dehydrogenation

Table 4 presents the results of cyclohexane dehydrogenation for the catalysts and physical mixtures. Benzene was the main product of the reaction, followed by traces of cyclohexene, as observed in the literature [47]. It was also verified that the α-Cr_2O_3 does not have activity for the dehydrogenation. The turnover number (TON) was calculated considering dissociative adsorption of O_2 in the chromium sites, expressed by the $O_2/Cr = 1:2$ ratio [48]. The results show that the TON is not constant, increasing as the chromium content increases. Thus, for supported chromium oxide catalysts the reaction is not structure-insensitive, unlike the behavior observed for supported noble metals [49]. A 10-factor between the lowest and the highest activity for samples of chromium on alumina is observed. The increase in the chromium particles aggregation increases the activity of the amorphous Cr^{3+} sites. In the Cr/SiO_2 catalysts, in spite of the detection of the α-Cr_2O_3 phase by XRD, the increase in the activity was also observed, ascribed to the amorphous Cr^{3+} aggregation.

The physical mixtures presented a typical behavior of catalyst, with the activity shifting likewise the catalysts in function of the chromium content. A TON range of 20-times was obtained for the physical mixtures with 2 and 13 wt.% Cr. However, the catalytic activity is mainly dependent of the dispersion of amorphous Cr^{3+} species.

3.2. Cr/SiO_2 catalysts for polymerization

3.2.1. Characterization

The catalysts, prepared with 1 wt.% Cr using different precursors (Table 1), were characterized by XRD, CO chemisorption and DRIFTS. In these catalysts, the α-Cr_2O_3 phase was not observed by XRD, after the calcination step, as it was for the Cr/SiO_2 catalysts prepared with chromium nitrate and loading of 1.5 wt.% Cr and higher. In our previous work [17], a fraction of amorphous Cr_2O_3 was observed in DR spectra for the 1CrBSi and 1CrCSi catalysts, while 1CrASi and 1CrDSi presented only Cr^{6+} after calcination. Therefore, distinct fractions of Cr^{6+} and Cr^{3+} were identified in the calcined form, depending on the chromium compound.

Preliminary tests with samples containing only Cr^{3+} or Cr^{6+} species in physical mixture were carried out in order to characterize the selectivity of CO chemisorption on Cr^{2+}, active sites for ethylene polymerization. The physical mixture of Cr_2O_3 in SiO_2 (3CrSiP3) did not present CO chemisorption, as well as the physical mixture of CrO_3 in SiO_2 (3CrSiP6), without previous reduction, and therefore presenting only Cr^{6+}. These results show that the technique is selective to characterize Cr^{2+}, since Cr^{6+} and Cr^{3+} species do not chemisorb CO.

Table 5
CO chemisorption, Cr^{2+} species distribution and ethylene polymerization results for supported Cr/SiO_2 catalysts and physical mixtures

Sample	Precursor	Chemisorption (μmol CO/g Cr)	Cr species distribution				Activity (g PE/g cat)
			Cr^{3+} (%)	Cr^{2+} (%)			
				Cr_A	Cr_B	Cr_C	
1CrASi	Acetate	2154	0	7.1	4.1	88.8	2430
1CrBSi	Silyl chromate	443	76	2.1	0.2	21.7	225
1CrCSi	Chloride	623	25	2.5	0.7	71.8	730
1CrDSi	CrO_3	2929	0	14.1	1.1	84.8	3007
3CrSiP6	CrO_3	325	0	1.1	0.6	98.3	NA[a]
3CrSiP3	Cr_2O_3	17	100	–	–	–	NA

[a] No activity.

Table 5 presents the distribution of chromium species after reduction with CO. The Cr^{2+} species distribution was based on CO chemisorption and DRIFTS analyses in the hydroxyls region of the spectrum. The bands at 3745, 3725 and 3600 cm^{-1} are ascribed to the isolated hydroxyls group [41], the Cr_B^{2+} and Cr_C^{2+} species interacting with the surface hydroxyls of the support, respectively [27]. In the calculation of the species distribution, we considered that the extinction coefficients of IR bands have the same order of magnitude and that the adsorption stoichometry ratio Cr^{2+}:CO is 1:1 [33,36]. The catalysts can be classified in decreasing order of Cr^{2+} (Cr_A^{2+} and Cr_B^{2+}) species: 1CrDSi > 1CrASi ≫ 1CrCSi > 1CrBSi, owing to its CO chemisorption results. These results are also related to the percentage of Cr^{3+}, obtained in previous TPR and DRS analyses, and in the complete reduction of the Cr^{6+} present for Cr^{2+} [17].

The 1CrASi and 1CrDSi catalysts, that presented only Cr^{6+} after the calcination and total reduction to Cr^{2+}, showed the highest values of CO chemisorption, presenting the largest fractions of Cr^{2+} active sites. The 1CrBSi and 1CrCSi catalysts presented the lowest amount of CO, also in agreement with the smaller percentage of Cr^{6+} in the calcined state and, therefore, smaller amount of Cr^{2+} sites after reduction. The largest chemisorption of CO in the 1CrDSi catalyst compared with the 1CrASi is associated to the largest fraction of $Cr_A^{2+} + Cr_B^{2+}$ active species than Cr_C^{2+}, that does not adsorb CO and it is not active in the polymerization.

The 3CrSiP6 physical mixture presented low CO chemisorption in contrast with the 1CrDSi catalyst, that was also prepared with CrO_3. However, the CO chemisorption of the physical mixture was similar to the obtained for the 1CrBSi catalyst, which presented smaller Cr^{2+} fraction. The lower CO chemisorption of the physical mixture can be ascribed to the largest fraction of Cr_C^{2+}.

Therefore, the 1CrASi and 1CrDSi catalysts presented the largest $Cr_A^{2+} + Cr_B^{2+}$ fractions. The 1CrBSi and 1CrCSi presented Cr^{2+} and Cr^{3+} species; this last one cannot be reduced by carbon monoxide and does not chemisorb CO. The fraction of Cr_A^{2+} was greater than the fraction of Cr_B^{2+} for all the samples. According to the literature [7], Cr_A^{2+} is transformed into Cr_C^{2+} at high temperatures under vacuum. This behavior is believed to be connected to the greater amount of Cr_B^{2+} than Cr_A^{2+} species for catalysts prepared with chromium acetate (1 and 3 wt.% Cr) in our previous work [18]. For these samples, we used a higher evacuation temperature (773 K) after reduction than in this work. Therefore, another important point is to compare the Cr^{2+} species distribution in the same treatment conditions.

3.2.2. Ethylene polymerization

The catalysts presented activities in the ethylene polymerization related to the amount of Cr_A^{2+} and Cr_B^{2+} active sites (Table 5). A correlation is observed between these parameters, resulting in two groups of catalysts in according to its activities: 1CrDSi/1CrASi and 1CrBSi/1CrCSi. The activity of the Cr_A^{2+} and Cr_B^{2+} sites was similar, since samples with distinct $Cr_A^{2+}/(Cr_A^{2+} + Cr_B^{2+})$ ratios, between 64 and

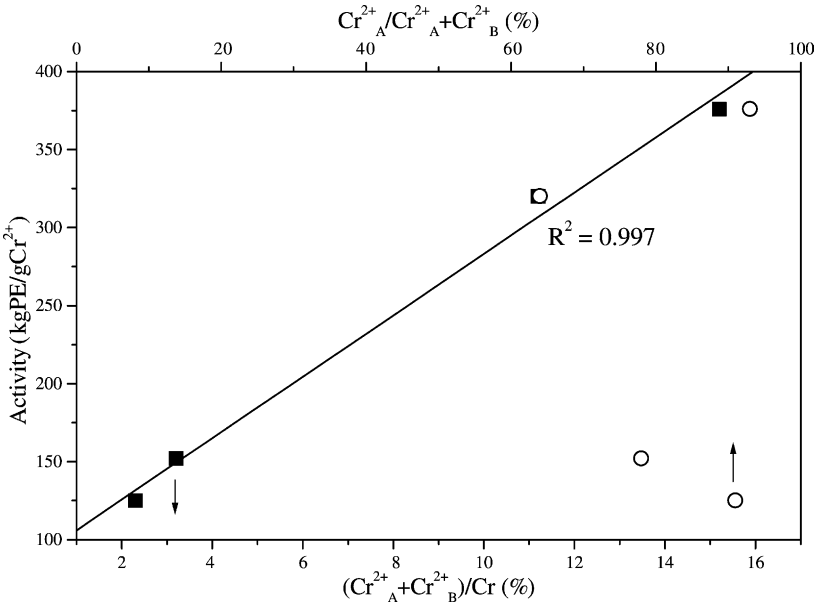

Fig. 11. Polymerization activity vs. $Cr^{2+}_A + Cr^{2+}_B$ species per chromium total (■) and $Cr^{2+}_A/(Cr^{2+}_A + Cr^{2+}_B)$ ratio (○).

93%, and total of active sites similar (Table 5) presented comparable polymerization activities, 320 and 376 kg PE/g Cr^{2+} (1CrASi and 1CrDSi, respectively). Thus, the ethylene polymerization is proportional to the total amount of Cr^{2+}_A and Cr^{2+}_B sites and the activity of these species is equivalent, as observed in Fig. 11. The CO chemisorption showed to be an important characterization technique to distinguish the Cr/SiO_2 catalysts in order to evaluate the activity in the ethylene polymerization.

The determination of the chromium species distribution and the activity of these species in the ethylene polymerization are very difficult due to the presence of distincts Cr^{2+} (of the types A, B and C) and of the Cr^{3+} species, which does not reduce and is inactive in the polymerization (Table 5). The difficult in obtaining the supported pure species of Cr^{2+} (Cr_A, Cr_B and Cr_C) as reference and the distinct characterization approaches hinder the results interpretations. Also contribute for the complexity of this system, the ease to oxidation of Cr^{2+} [34] and the change in the Cr^{2+} species distribution, due to distinct condition of preparation and pretreatment [7]. Besides, chromium catalysts for polymerization have total amount of metal around 1 wt.% Cr. This low content makes difficult the quantification of chromium active sites.

4. Conclusions

The selectivity of the O_2 and CO chemisorption to characterize the Cr^{2+} and amorphous Cr^{3+} sites, respectively, was verified. It was observed correlation between the O_2 and CO chemisorptions and the activities for the dehydrogenation and polymerization reactions, respectively.

Alumina disperses chromium particles in its surface better than silica. This phenomena is driven by the surface hydroxyls distribution and, probably, by the affinity between the crystallographic orientation of α-Cr_2O_3 and of the support. Physical mixtures of CrO_3 with alumina present activity in the dehydrogenation in the same extent to the obtained with the catalysts, ascribed to a spontaneous spreading process of the chromium oxide(VI).

The cyclohexane dehydrogenation reaction showed to be structure-sensitive for chromium catalysts. The activity was favored by the chromium particles agglomeration. The activity of the Cr/SiO_2 catalysts

to the ethylene polymerization is associated to the amount of $Cr_A^{2+} + Cr_B^{2+}$ species. These chromium species present similar activities in the polymerization.

Acknowledgements

A.B. Gaspar and J.L.F. Brito are grateful to CNPq (Conselho Nacional de Desenvolvimento Científico e Tecnológico, Brasil) for the scholarship received during this work.

References

[1] F. Cavani, M. Koutyrev, F. Trifiro, A. Bartolini, D. Ghisletti, R. Iezzi, A. Santucci, G. Del Piero, J. Catal. 158 (1996) 236.
[2] B.M. Weckhuysen, R.A. Schoonheydt, Catal. Today 51 (1999) 215.
[3] B.M. Weckhuysen, R.A. Schoonheydt, Catal. Today 51 (1999) 223.
[4] J.P. Hogan, J. Polym. Sci. A-1 8 (1970) 2637.
[5] M.P. McDaniel, Adv. Catal. 33 (1985) 47.
[6] A. Zecchina, G. Spoto, G. Ghiotti, E. Garrone, J. Mol. Catal. 86 (1994) 423.
[7] E. Garrone, G. Ghiotti, A. Zecchina, in: Y. Imamoglu (Ed.), Olefin Metathesis and Polymerization Catalysts, Kluwer academic Publishers, Amsterdam, 1990, p. 393.
[8] G. Ghiotti, E. Garrone, A. Zecchina, J. Mol. Catal. 46 (1988) 61.
[9] K. Vikulov, G. Spoto, S. Coluccia, A. Zecchina, Catal. Lett. 16 (1992) 117.
[10] B.M. Weckhuysen, A. Bensalem, R.A. Schoonheydt, J. Chem. Soc., Faraday Trans. 94 (1998) 2011.
[11] S. De Rossi, G. Ferraris, S. Fremiotti, A. Cimino, V. Indovina, Appl. Catal. 81 (1992) 113.
[12] K.S. Rama Rao, K.V. Narayana, A. Venogupal, V. Venkat Rao, S. Khaja Masthan, P. Kanta Rao, Indian J. Chem. 35 (1996) 656.
[13] M.P. McDaniel, M.B. Welch, J. Catal. 82 (1983) 98.
[14] M.P. McDaniel, J. Catal. 76 (1982) 37.
[15] I.V. Babich, Y.V. Plyuto, O. Van der Voort, E.F. Vansant, J. Coll. Inter. Sci. 189 (1997) 144.
[16] V.J. Ruddick, P.W. Dyer, G. Bell, V. C Gibson, J.P.S. Badyal, J. Phys. Chem. 100 (1996) 11062.
[17] A.B. Gaspar, L.C. Dieguez, Appl. Catal. 227 (2002) 241.
[18] A.B. Gaspar, R.L. Martins, M. Schmal, L.C. Dieguez, J. Mol. Catal. 169 (2001) 105.
[19] M.A. Vuurman, I.E. Wachs, D.J. Stufkens, A. Oskam, J. Mol. Catal. 80 (1993) 209.
[20] M.D. Einarson, D.M. Mackay, Environ. Sci. Technol. 35 (3) (2001) 67.
[21] C. Hogue, Chem. Eng. News 8 (2000) 40.
[22] M.L. Morgan, in: W. Keim, B. Lücke, J. Weitkamp (Eds.) Proceedings of the DGMK Conference on C_4 Chemistry—Manufacture and Use of C_4 Hydrocarbons, Tagungsbericht 9705, Germany, 1997, p. 9.
[23] N.O. Elbashir, S.M. Al-Zahrani, A.E. Abasaeed, M. Abdulwahed, Chem. Eng. Proc. 42 (2003) 817.
[24] G. Karamullaoglu, S. Onen, T. Dogu, Chem. Eng. Proc. 41 (2002) 337.
[25] B. Grzybowska, J. Słoczyński, R. Grabowski, L. Keromnes, K. Wcisło, T. Bobińska, Appl. Catal. 209 (2001) 279.
[26] S. De Rossi, M.P. Casaletto, G. Ferraris, A. Cimino, G. Minelli, Appl. Catal. 167 (1998) 257.
[27] C.S. Kim, S.I. Woo, J. Mol. Catal. 73 (1992) 249.
[28] H.L. Krauss, H.Z. Stach, Z. Anorg. Allg. Chem. 366 (1969) 280.
[29] A. Rahman, M.H. Mohamed, M. Ahmed, A.M. Aitani, Appl. Catal. 121 (1995) 203.
[30] B. Liu, M. Terano, J. Mol. Catal. 172 (2001) 227.
[31] B. Liu, H. Nakatani, M. Terano, J. Mol. Catal. 184 (2002) 387.
[32] S.W. Weller, Acc. Chem. Res. 16 (1983) 106.
[33] A. Zecchina, E. Garrone, G. Ghiotti, S. Coluccia, J. Phys. Chem. 79 (1975) 972.
[34] M.P. McDaniel, S.J. Martin, J. Phys. Chem. 95 (1991) 3289.
[35] M. Kantcheva, I.G. Dalla Lana, J.A. Szymura, J. Catal. 154 (1995) 329.
[36] C. Groeneveld, P.P.M.M. Wittgen, H.P. Swinnen, A. Wernsen, G.C.A. Schuit, J. Catal. 83 (1983) 346.
[37] L.M. Baker, W.L. Carrick, J. Org. Chem. 35 (1970) 774.
[38] R. Merryfield, M.P. McDaniel, G. Parks, J. Catal. 77 (1982) 348.
[39] F.D. Hardcastle, I.E. Wachs, J. Mol. Catal. 46 (1988) 173.
[40] M.A. Vuurman, F.D. Hardcastle, I.E. Wachs, J. Mol. Catal. 84 (1993) 193.
[41] R.K. Iler, The Chemistry of Silica, Wiley, New York, 1979.
[42] H. Knözinger, P. Ratnasamy, Catal. Rev. Sci. Eng. 17 (1978) 31.
[43] A. Ellison, T.L. Overton, L. Benzce, J. Chem. Soc., Faraday Trans. 89 (1993) 843.
[44] P.A. Webb, C. Orr, Analytical Methods in Fine Particle Technology, Micromeritcs, Norcross, GA, 1997, p. 227.
[45] A. Baiker, Int. Chem. Eng. 25 (1985) 16.
[46] R.C. Weast, in: M. Astle, W. Beyer (Eds.), Handbook of Chemistry and Physics, 66th ed., The Chemical Rubber Co., Cleveland, OH, 1985.
[47] K. Jagannathan, A. Srinivasan, C.N.R. Rao, J. Catal. 69 (1981) 418.
[48] D.A. King, D.P. Woodruff, in: The Chemical Physics of Solid Surface and Heterogeneous Catalysts: Chemisorption Systems, part A, vol. 3, Elsevier, Amsterdam, 1990, p. 140.
[49] M. Boudart, Adv. Catal. 20 (1969) 153.